

УДК 539.12.01

## NOVEL APPLICATIONS OF GROUP THEORY IN NUCLEAR PHYSICS

*J. P. Draayer*<sup>a</sup>, *J. G. Hirsch*<sup>b</sup>, *G. Popa*<sup>c</sup>, *Feng Pan*<sup>a,d</sup>,  
*G. Stoitcheva*<sup>a</sup>, *A. I. Georgieva*<sup>e</sup>, *K. D. Sviratcheva*<sup>a</sup>

<sup>a</sup>Louisiana State University, Department of Physics and Astronomy,  
Baton Rouge, Louisiana, USA

<sup>b</sup>Instituto de Ciencias Nucleares, Universidad Nacional Autónoma de México, México

<sup>c</sup>Department of Physics, Rochester Institute of Technology,  
Rochester, New York, USA

<sup>d</sup>Department of Physics, Liaoning Normal University, Dalian, China

<sup>e</sup>Institute of Nuclear Research and Nuclear Energy,  
Bulgarian Academy of Sciences, Sofia, Bulgaria

A general procedure, based on the Bethe ansatz, is proposed for finding algebraic solutions for low-lying  $J=0$  states of  $2k$  nucleons interacting with one another through a  $T=1$  charge independent pairing interaction. Results provided by Richardson are shown to be valid for up to two pairs,  $k \leq 2$ ; we gave expressions for up to three pairs,  $k \leq 3$ . The results shown that a set of highly nonlinear equations must be solved for  $3k \geq 3$ .

### INTRODUCTION

While large-scale shell-model calculations are useful for reproducing experimental data, insight into the physical underpinnings of many-body quantum phenomena, such as the structure of atomic nuclei, requires a deeper understanding of underlying principles that can only be achieved through a study of the system's symmetries, those underlying properties that dictate its gross structure.

In this article we review some recent novel algebraic approaches used to explore special features of atomic nuclei: quadrupole collectivity and the scissors mode as revealed through  $SU(3)$  [1]; and exact solutions for the pairing problem via the Bethe ansatz and infinite-dimensional group algebras [2]. The use of deformed algebraic structures to predict binding energies of exotic nuclei is covered in a companion article [3]. Important recent work on the latter can also be found in [4,5].

## 1. QUADRUPOLE COLLECTIVITY AND THE SCISSORS MODE IN DEFORMED NUCLEI

Experimental nuclear physicists continue to challenge theorists with interesting new observations. Measurements of new levels, some lying below 3 MeV, raise questions about the nature of collective excitations in atomic nuclei. Heavy deformed nuclei with  $A \geq 150$  are good candidates for probing these degrees of freedom. It follows that microscopic calculations for these nuclei are important for gaining a deeper understanding of the corresponding structures. Of special interest, for example, is the nature of excited  $0^+$  bands and the fragmentation of the ground state  $M1$  strength distribution [6–10].

The pseudo- $SU_3$  model is a tool that can be used to probe the microscopic nature of collective phenomena in heavy deformed nuclei. Recent results have been reported for the  $^{160,162,164}\text{Dy}$  and  $^{168}\text{Er}$  nuclei [11]. These nuclei, as for the Gd isotopes studied earlier [12], exhibit well-developed ground-state rotational bands as well as states that are associated with excited low-lying  $K^\pi = 0^+$  and  $K^\pi = 2^+$  bands. Here we give an overview of an application of the pseudo- $SU_3$  model in these cases; in particular, we will focus on its ability to make reasonable predictions for observed low-lying  $1^+$  states, the ground-state  $M1$  sum rule and its corresponding energy-weighted centroid, and the observed fragmentation of this  $M1$  strength. The results will illustrate how this particular «novel» application of group theory leads to a much deeper understanding of a complex microscopic phenomena in nuclear physics.

**1.1. Model Space and Hamiltonian Parameters.** Rare earth nuclei are considered to have closed shells at  $N_\pi = 50$  for protons and  $N_\nu = 82$  for neutrons. To build basis states we considered the following open shells:  $\eta_\pi = 4$  for protons and  $\eta_\nu = 5$  for neutrons along with their intruder state complements,  $h_{11/2}$  for protons and  $i_{13/2}$  for neutrons, even though particles in these unique-parity intruder levels are only considered to renormalize the normal-parity configurations through the use of an effective charge. These oscillator shells have a complementary pseudo-harmonic oscillator shell structure given by  $\tilde{\eta}_\sigma$  ( $\sigma = \pi, \nu$ ) =  $\eta_\sigma - 1$ . Approximately 20 pseudo- $SU_3$  irreducible representation (irreps) with the largest values for the second order Casimir operator ( $C_2$  where  $Q \cdot Q = 4C_2 - 3L^2$ ), were used to build the basis states.

The pseudo- $SU_3$  Hamiltonian used in the analysis is given by:

$$H = H_{\text{sp}}^\pi + H_{\text{sp}}^\nu - \frac{1}{2}\chi Q \cdot Q - G_\pi H_P^\pi - G_\nu H_P^\nu + \\ + aJ^2 + bK_J^2 + a_3C_3 + a_{\text{sym}}C_2. \quad (1)$$

Strengths of the quadrupole-quadrupole ( $Q \cdot Q$ ) and pairing interactions ( $H_P^\sigma$ ) were fixed, respectively, at values typical of those used by other authors, namely,

Table 1. Parameters of the pseudo- $SU_3$  Hamiltonian

Parameter	$^{168}\text{Er}$	$^{164}\text{Dy}$	$^{162}\text{Dy}$	$^{160}\text{Dy}$
$\hbar\omega$	7.40	7.49	7.52	7.55
$\chi \cdot 10^{-3}$	6.84	7.12	7.27	7.42
$D_\pi$	-0.283	-0.286	-0.287	-0.289
$D_\nu$	-0.198	-0.200	-0.201	-0.202
$G_\pi$	0.125	0.128	0.130	0.131
$G_\nu$	0.101	0.104	0.105	0.106
$a \cdot 10^{-3}$	-2.1	-2.0	0.0	1.0
$b$	0.022	0.00	0.08	0.10
$a_{\text{sym}} \cdot 10^{-3}$	0.80	1.20	1.40	1.45
$a_3 \cdot 10^{-4}$	0.75	0.65	1.32	1.36

$\chi = 35 A^{5/3}$  MeV,  $G_\pi = 21/A$  MeV and  $G_\nu = 19/A$  MeV. The spherical single-particle terms in this expression have the form

$$H_{\text{sp}}^\sigma = \sum_{i_\sigma} (C_\sigma \mathbf{l}_{i_\sigma} \cdot \mathbf{s}_{i_\sigma} + D_\sigma \mathbf{l}_{i_\sigma}^2). \quad (2)$$

Since only pseudo-spin zero states were considered, matrix elements of the spin-orbit part of this interaction vanish identically. Calculations were carried out under the assumption that the single-particle orbit-orbit ( $l^2$ ) interaction strengths were fixed by systematics [13],  $D_\sigma (\sigma = \pi, \nu) = \hbar\omega \kappa_\sigma \mu_\sigma$ ,  $\hbar\omega = 41/A^{1/3}$  with  $\kappa_\sigma$  and  $\mu_\sigma$  assigned their usual oscillator values [13], namely,  $\kappa_\pi = 0.0637$ ,  $\mu_\pi = 0.60$ ;  $\kappa_\nu = 0.0637$ ,  $\mu_\nu = 0.42$ .

Relative excitation energies for states with angular momentum  $0^+$  are determined mainly by the quadrupole-quadrupole interaction. The single-particle terms and pairing interactions mix these states. With the strength of these interactions fixed as in Table 1, the  $0_2^+$  states lie very close to their experimental counterparts while the  $0_3^+$  states usually lie slightly above the experimental ones. Of the four «free» parameters in the Hamiltonian,  $a$  was adjusted to reproduce the moment of inertia of the ground state band,  $a_3$  was varied to yield a best fit to the energy of the second  $0^+$  state (the energy of the third  $0^+$  was not included in the fitting and as the results given below show these all fall slightly higher than their experimental counterparts),  $a_{\text{sym}}$  was adjusted to give a best fit to the first  $1^+$  state, and  $b$  was fit to the value of the band-head energy of the  $K^\pi = 2^+$  band.

In the rotational model the projection  $K$  of angular momentum on the body-fixed symmetry axis is a good quantum number. For each intrinsic state with a given value of  $K$  there is a set of levels with  $L = K, K + 1, K + 2, \dots$ , except for  $K = 0$  when  $L$  is either even or odd depending on the intrinsic ( $D_2$ )

symmetry of the configuration. Elliott [14] used group-theoretical methods to investigate classification schemes for particles in a three-dimensional harmonic oscillator potential for which the underlying symmetry is  $SU_3$ . He noted that the angular momenta in an irrep of  $SU_3$  can be grouped in a similar way to that of the rotor, the differences being that there are a fixed number of  $K$  values and that each band supports a finite number of  $L$  values rather than being of infinite length. The angular momentum content of an  $SU_3$  irrep  $(\lambda, \mu)$  can be sorted into  $K$  bands according to the following rule [15]:  $K = \min(\lambda, \mu), \min(\lambda, \mu) - 2, \dots, 1$  or  $0$ , where  $L = (\lambda + \mu), (\lambda + \mu) - 2, \dots, 1$  or  $0$  for  $K = 0$  and  $L = K, K + 1, K + 2, \dots, (\lambda + \mu) - K + 1$  for  $K \neq 0$ . Hence, for  $^{160}\text{Dy}$  with leading  $SU_3$  irrep (28,8) we have  $L = 0, 2, \dots, 36$  for the  $K = 0$  band,  $L = 2, 3, \dots, 35$  for the  $K = 2$  band, etc.

**1.2. Applications —  $B(E2)$  and  $B(M1)$  Transition Strengths.** Theoretical and experimental [16]  $B(E2)$  transition strengths between the states in the ground state band in  $^{162}\text{Dy}$  are shown in Table 2. The agreement between the calculated and experimental numbers is excellent. The  $B(E2; 2_1 \rightarrow 4_1)$  is equal to within 1% of the experimental value, and the last two calculated  $B(E2)$  values differ from the experimental values by less than  $0.1 \text{ e}^2 \cdot \text{b}^2$  which is well within the experimental error. Excellent agreement with experimental  $B(E2)$  data is also observed in  $^{162}\text{Dy}$  and  $^{164}\text{Dy}$ . Contributions to the quadrupole moments from the nucleons in the unique parity orbitals are parameterized through an effective charge [15],  $e_f$ , with  $e_\nu = e_f$ , and  $e_\pi = 1 + e_f$ , so the  $E2$  operator is given by [15]:  $Q_\mu = e_\pi Q_\pi + e_\nu Q_\nu$ .

Table 2. Experimental and theoretical  $B(E2)$  transition strengths between members of ground state band of  $^{162}\text{Dy}$

$J_i \rightarrow J_f$	$B(E2; J_i \rightarrow J_f), \text{e}^2 \cdot \text{b}^2$	
	Exp.	Theory
$0_1 \rightarrow 2_1$	$5.134 \pm 0.155$	5.134
$2_1 \rightarrow 4_1$	$2.675 \pm 0.102$	2.635
$4_1 \rightarrow 6_1$	$2.236 \pm 0.127$	2.325
$6_1 \rightarrow 8_1$	$2.341 \pm 0.115$	2.201

Theoretical intraband  $B(E2)$  transition strengths between the states in the  $K = 2$  and the first and second excited  $K = 0$  bands are given in Table 3. Note that the strengths of the transition probabilities are consistent across all four bands (Tables 2 and 3).

Another test for the theory is the  $M1$  transition strength distributions that can be obtained using eigenvectors of the diagonalized Hamiltonian (1). The calculated and experimental  $M1$  strength distributions for the Dy nuclei are given

in Fig. 1. For illustrative purposes, the energies and  $M1$  transition spectra are given opposite one another.

**Table 3. Theoretical  $B(E2)$  transition strengths between states of the  $K = 2$ ,  $K = 0_2$ , and  $K = 0_3$  bands of  $^{162}\text{Dy}$ . The energies are labeled with the subindex  $\gamma$  for the  $K = 2$  band,  $a$ , and  $b$  for the first and second excited  $K = 0$  bands**

$K = 2$		$K = 0_2$		$K = 0_3$	
$2_\gamma \rightarrow 3_\gamma$	2.480	$0_a \rightarrow 2_a$	4.193	$0_b \rightarrow 2_b$	3.517
$2_\gamma \rightarrow 4_\gamma$	1.060	$2_a \rightarrow 4_a$	2.272	$2_b \rightarrow 4_b$	1.901
$3_\gamma \rightarrow 4_\gamma$	1.630	$4_a \rightarrow 6_a$	2.153	$4_b \rightarrow 6_b$	2.017
$4_\gamma \rightarrow 5_\gamma$	1.145	$6_a \rightarrow 8_a$	2.175	$6_b \rightarrow 8_b$	2.030
$4_\gamma \rightarrow 6_\gamma$	1.625				
$5_\gamma \rightarrow 6_\gamma$	0.716				
$6_\gamma \rightarrow 7_\gamma$	0.607				
$6_\gamma \rightarrow 8_\gamma$	1.685				

**Table 4. Total  $B(M1)$  strength from experiment [16] and the present calculation**

Nucleus	$\sum B(M1), \mu_N^2$		
	Experiment	Calculated	
		Pure $SU_3$	Theory
$^{160}\text{Dy}$	2.48	4.24	2.32
$^{162}\text{Dy}$	3.29	4.24	2.29
$^{164}\text{Dy}$	5.63	4.36	3.05

The starting point for a geometric interpretation of the scissors mode within the framework of the  $SU_3$  shell model is the well-known relation of the  $SU_3$  symmetry group to  $\text{Rot}(3)$ , the symmetry group of the rotor [17, 18]. The structure of the intrinsic Hamiltonian allows for a rotor-model interpretation of the coupled  $SU_3$  irreps  $(\lambda_\pi, \mu_\pi)$  and  $(\lambda_\nu, \mu_\nu)$  for protons and neutrons, respectively. According to the Littlewood rules [19] for coupling Young diagrams, the allowed product configuration can be expressed in mathematical terms by using three integers  $(m, l, k)$ :  $(\lambda_\pi, \mu_\pi) \otimes (\lambda_\nu, \mu_\nu) = \oplus_{m,l,k} (\lambda_\pi + \lambda_\nu - 2m + l, \mu_\pi + \mu_\nu - 2l + m)^k$ , where the parameters  $l$  and  $m$  are defined in a fixed range given by the values of the initial  $SU_3$  representations. In this formulation,  $k$  serves to distinguish between multiple occurrences of equivalent  $(\lambda, \mu)$  irreps in the tensor product. The number of  $k$  values is equal to the outer multiplicity,  $\rho_{\max}$  ( $k = 1, 2, \dots, \rho_{\max}$ ).

The  $l$  and  $m$  labels in this formulation can be identified [20] with excitation quanta of a two-dimensional oscillator involving relative rotations ( $\theta$ , the angle between the principal axes of the proton and neutron system, and  $\phi$ , the angle

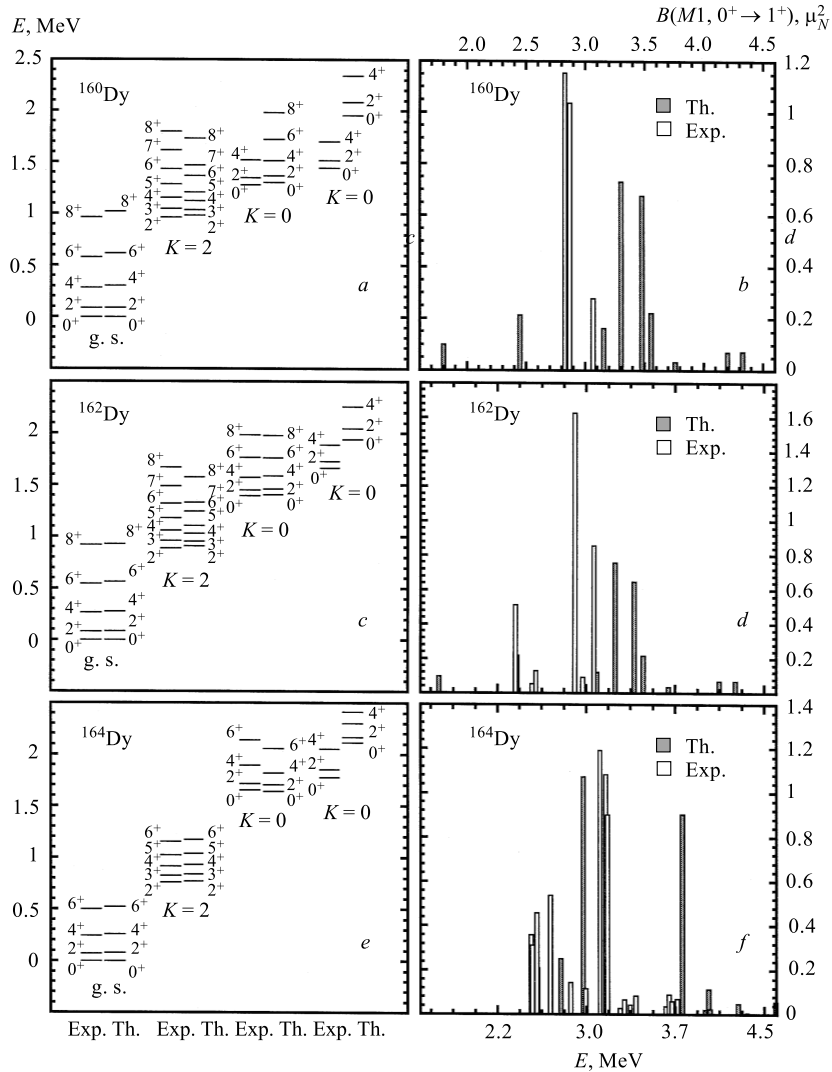


Fig. 1. Energy spectra of  $^{160}\text{Dy}$ ,  $^{162}\text{Dy}$ , and  $^{164}\text{Dy}$  obtained using Hamiltonian (1). «Exp.» represents the experimental results and «Th.» the calculated ones. Figures *b*, *d*, and *f* give the theoretical and experimental  $M1$  transition strengths from the  $J = 0$  ground state to various  $J = 1$  states

between semiaxes of the proton and neutron system) of the proton–neutron system,  $m = n_\theta, l = n_\phi$ . These correspond to two distinct types of  $1^+$  motion, the scissors and twist modes, and their realization in terms of the pseudo- $SU_3$  model.

The  $SU_3$  irreps obtained from the tensor product that contain a  $J^\pi = 1^+$  state are those corresponding to  $(m, l, k) = (1, 0, 1)$ ,  $(0, 1, 1)$ ,  $(1, 1, 1)$ , and  $(1, 1, 2)$ . A pure  $SU_3$  picture gives rise of a maximum of four  $1^+$  states that are associated with the scissors, twist, and double degenerate scissors-plus-twist modes  $[(1,1,1)$  and  $(1,1,2)]$  [20]. Results for the Dy isotopes, assuming a pure pseudo- $SU_3$  scheme, are given in Table 6.

*Table 5.  $B(M1)$  transition strengths ( $\mu_N^2$ ) in the pure symmetry limit of the pseudo- $SU_3$  model. The strong coupled pseudo- $SU_3$  irrep  $(\lambda, \mu)_{gs}$  for the ground state is given with its proton and neutron subirreps and the irreps associated with the  $1^+$  states,  $(\lambda', \mu')_{1^+}$ . In addition, each transition is labeled as a scissors (s), or twist (t), or combination mode*

Nucleus	$[(\lambda_\pi, \mu_\pi)$	$(\lambda_\pi, \mu_\pi)$	$(\lambda, \mu)_{gs}$	$(\lambda, \mu)_{1^+}$	$B(M1)$	Mode
$^{160,162}\text{Dy}$	(10, 4)	(18, 4)	(28, 8)	(29, 6)	0.56	t
				(26, 9)	1.77	s
				$(27, 7)^1$	1.82	s + t
				$(27, 7)^2$	0.083	t + s
$^{164}\text{Dy}$	(10, 4)	(20, 4)	(30, 8)	(31, 6)	0.56	t
				(28, 9)	1.83	s
				(29, 7)	1.88	s + t
				(29, 7)	0.09	t + s

The experimental results [16] given in Fig. 1, *b, d, f* suggest a much larger number of  $1^+$  states with nonzero  $M1$  transition probabilities from the  $0^+$  ground state. The  $SU_3$  breaking residual interactions lead to a fragmentation in the  $M1$  strength distribution, since the ground state  $0^+$  is in that case a combination of several  $SU_3$  irreps, each will allow  $M1$  transitions to other  $SU_3$  irreps. Overall, the total  $M1$  strength is in reasonable agreement with the experimental results (Table 4). In  $^{164}\text{Dy}$  the total  $M1$  strength is slightly underestimated, which may be due to spin admixtures in the wave function, which is not included in this work.

**1.3. Conclusions Regarding «Novel» Pseudo- $SU(3)$  Applications.** This study of  $^{160,162,164}\text{Dy}$  shows that pseudo-spin zero neutron and proton configuration with a relatively few pseudo- $SU_3$  irreps with the largest  $C_2$  values suffices to obtain good agreement with known experimental results. The Hamiltonian that was used included single-particle energies, the quadrupole–quadrupole interaction, and neutron and proton pairing terms, all with strengths fixed by systematics, plus four smaller rotor-like terms with strengths that were varied to maximize agreement with observations. A consistent set of «free» parameters was obtained. The results generated extended beyond quantities that were used in the fitting procedure, including intraband  $B(E2)$  strengths and the  $M1$  strength distribution of the ground state (Table 5).

The  $M1$  strength distributions were not fit to the data. Nevertheless, in all cases the summed strength was found to be in good agreement with the experiment numbers. The pseudo- $SU_3$  model therefore offers a microscopic shell-model interpretation of the «scissors» mode [21], and in addition, it reveals a «twist» degree of freedom that corresponds to allowed relative angular motion of the proton and/or neutron subdistribution [20]. By adding one-body and two-body pairing interactions to the Hamiltonian, it was possible to describe the experimentally observed fragmentation of the  $M1$  strength. The results suggest that more detailed microscopic description of other properties of heavy deformed nuclei, such as  $g$  factors and beta decay, may finally be within reach of a bona fide microscopic theory. In summary one can certainly say that the  $SU(3)$  picture yields a «novel» twist to the concept of the scissors mode in deformed nuclei!

## 2. PAIRING CORRELATIONS AND NOVEL ALGEBRAIC STRUCTURES

Pairing is an important residual interaction in nuclear physics [22–25]. Typically, after adopting a mean-field approach, the pairing interaction is treated approximately using either Bardeen–Cooper–Schrieffer (BCS) or Hartree–Fock–Bogoliubov (HFB) methods, sometimes in conjunction with correction terms evaluated within the Random-Phase Approximation (RPA). However, both the BCS and HFB approximations suffer from serious deficiencies such as the particle number nonconservation. While remedies may exist, often they do not yield better physics — such is the case for higher-lying excited states in nuclear physics that are a natural part of the spectrum of the pairing Hamiltonian.

Exact solutions of the mean-field plus pairing model were first studied for the equal strength pairing model [26]. Recently, generalizations that include state dependent pairing have been considered. In these cases, the Bethe ansatz has been evoked, from which excitation energies and the corresponding wave functions can be determined through a set of nonlinear equations. This particular «novel» application of group theory involves the use of an infinite-dimensional algebra. While solving these nonlinear equations is not always practical when the number of levels and valence nucleon pairs are large, which applies for well-deformed nuclei, the method can be used to explore the role of pairing correlations in lighter systems [27–29]. As is well known, an equal strength pairing interaction, which is used in many applications, is not a particularly good approximation for well-deformed nuclei. In order to study pairing interactions for well-deformed nuclei, a hard-core Bose–Hubbard model was adopted, which is equivalent to a mean-field plus nearest-level pairing theory [2]. This model is also exactly solvable, and is applied to describe well-deformed nuclei in the rare-earth and actinide regions.

**2.1. New Algebraic Bethe Ansatz Approach.** The general pairing Hamiltonian for spherical nuclei can be written as

$$\hat{H} = \sum_{jm} \varepsilon_j a_{jm}^\dagger a_{jm} - \sum_{jj'} c_{jj'} S^+(j) S^-(j'), \quad (3)$$

where the  $\varepsilon_j$  are single-particle energies and  $S^\pm(j)$  and  $S^0(j)$  are the pairing operators for a single- $j$  shell, and  $c_{jj'}$  is the strength of the pairing interaction between the  $j$  and  $j'$  shells. In nondegenerate cases,  $\varepsilon_j$  are real numbers that are not equal to each other. In this case one can assume that the parameters  $c_{jj'}$  can be expanded in terms of the  $\varepsilon_j$  as  $c_{jj'} = \sum_{mn} g_{mn} \varepsilon_j^m \varepsilon_{j'}^n$ , where  $\{g_{mn}\}$  is a set of parameters to be determined. Hence, similarly to the separable pairing case [27–29], we introduce the operators  $\{S_n^\mu; \mu = 0, +, -; n = 0, 1, 2, \dots\}$  with

$$S_n^+ = \sum_j \varepsilon_j^n S^+(j), \quad S_n^- = \sum_j \varepsilon_j^n S^-(j), \quad S_n^0 = \sum_j \varepsilon_j^n S^0(j). \quad (4)$$

The operators  $\{S_n^\mu\}$ , which form a half-positive infinite-dimensional Lie algebra  $\widehat{SU(2)}$  without central extension, satisfy the following commutation relations:

$$[S_m^+, S_n^-] = 2S_{m+n}^0, \quad [S^0, S^\pm] = \pm S_{m+n}^\pm. \quad (5)$$

Using these  $\widehat{SU(2)}$  generators, one can rewrite the Hamiltonian (3) as

$$\hat{H} = \sum_j \varepsilon_j \Omega_j + 2S_1^0 - \sum_{mn} g_{mn} S_m^+ S_n^-, \quad (6)$$

where  $\Omega_j = (2j + 1)/2$ . In order to diagonalize the Hamiltonian (6), we use the following Bethe ansatz wave function:

$$|k; \zeta\rangle = \mathcal{N} S^+(x_1^{(\zeta)}) S^+(x_2^{(\zeta)}) \dots S^+(x_k^{(\zeta)}) |0\rangle, \quad (7)$$

where  $\mathcal{N}$  is a normalization constant;  $\zeta$  is an additional quantum number used to distinguish different eigenstates with the same number of pairs  $k$ , and  $|0\rangle$  is the pairing vacuum state,

$$S^+(x_r^{(\zeta)}) = \sum_m a_m S_m^+(x_r^{(\zeta)}) \quad (8)$$

in which  $\{a_m\}$  and  $\{x_r^{(\zeta)}\}$  are two sets of  $c$  numbers to be determined and

$$S_m^+(x_r^{(\zeta)}) = \sum_j \frac{\varepsilon_j^m}{1 - \varepsilon_j x_r^{(\zeta)}} S_j^+. \quad (9)$$

In solving the corresponding eigenvalue equation we observe that like the separable pairing case [28], auxiliary conditions are necessary to cancel the so-called unwanted terms, and these can be chosen as

$$\sum_{\nu} a_{\nu} \varepsilon_j^{\nu} G_{ij} = \sum_s \frac{c_s^{(i)}(r, q)}{1 - \varepsilon_j z_s^{(i)}(r, q)}, \quad (10)$$

where  $\{c_s^{(i)}(r, q)\}$  and  $\{z_s^{(i)}(r, q)\}$  are two other sets of unknown  $c$  numbers to be determined and  $G_{nj} = \sum_m g_{nm} \varepsilon_j^m$ . One can prove that the  $k$ -pair eigenenergies are given by

$$E_k^{(\zeta)} = \sum_{i=1}^k \frac{2}{x_i^{(\zeta)}}. \quad (11)$$

Furthermore, the  $c$  numbers  $\{a_m\}$  ( $m = 0, 1, \dots, p-1$ ),  $\{x_r^{(\zeta)}\}$  ( $r = 1, 2, \dots, k$ ),  $\{c_s^{(i)}(r, q)\}$  and  $\{z_s^{(i)}(r, q)\}$  ( $0 \leq i, s \leq p-1$ ,  $1 \leq r \neq q \leq k$ ) must satisfy

$$\frac{a_i}{x_{\mu}^{(\zeta)}} = \Lambda_i(x_{\mu}^{(\zeta)}) + \sum_{\nu \neq \mu} \frac{x_{\nu}^{(\zeta)}}{x_{\nu}^{(\zeta)} - x_{\mu}^{(\zeta)}} \mathcal{A}_i^{\mu}(x_{\nu}^{(\zeta)}) \quad (12)$$

and

$$\begin{aligned} \sum_s \frac{c_s^{(i)}(r, q) (z_s^{(i)}(r, q))^2}{(1 - \varepsilon_j z_s^{(i)}(r, q)) (z_s^{(i)}(r, q) - x_r^{(\zeta)}) (z_s^{(i)}(r, q) - x_q^{(\zeta)})} &= \\ &= \frac{a_i}{(1 - \varepsilon_j x_r^{(\zeta)}) (1 - \varepsilon_j x_q^{(\zeta)})} \end{aligned} \quad (13)$$

for fixed  $j$ ,  $i$ , and  $r \neq q$ , where

$$\Lambda_m(x) = \sum_{n\mu} \langle S_{\mu+n}^0(x) \rangle a_{\mu} g_{mn} \quad (14)$$

with

$$\langle S_{\mu+n}^0(x) \rangle = \frac{1}{2} \sum_j \frac{\varepsilon_j^{\nu} (\tau - \Omega_j)}{1 - \varepsilon_j x}, \quad (15)$$

$\tau = \sum_j \tau_j$  is the seniority quantum number of the pairing vacuum and

$$\mathcal{A}_i^{\mu}(x_{\nu}) = a_i - \sum_s \frac{c_s^{(i)}(\mu, \nu) x_{\nu}}{z_s^{(i)}(\mu, \nu) - x_{\nu}}. \quad (16)$$

As a simple example of the theory, we consider the  $J = 0$  pairing of the even-even oxygen isotopes  $^{18-26}\text{O}$ . The neutron single-particle energies  $\varepsilon_j$  are taken from the energy spectra of  $^{17}\text{O}$  with  $\varepsilon_{1/2} = -3.273$ ,  $\varepsilon_{3/2} = 0.941$ , and  $\varepsilon_{5/2} = -4.143$  MeV. These values are all relative to the binding energy of  $^{16}\text{O}$ , which is taken to be zero. The two-body general pairing strengths  $c_{jj'}$  in MeV are taken from the  $J = 0$  two-body matrix elements of the universal  $ds$ -shell Hamiltonian [30] with  $c_{\frac{1}{2}\frac{1}{2}} = 2.125$ ,  $c_{\frac{3}{2}\frac{3}{2}} = 1.092$ ,  $c_{\frac{5}{2}\frac{5}{2}} = 0.940$ ,  $c_{\frac{1}{2}\frac{3}{2}} = 0.766$ ,  $c_{\frac{1}{2}\frac{5}{2}} = 0.765$ , and  $c_{\frac{3}{2}\frac{5}{2}} = 1.301$ . Using these data, we have calculated the pairing excitation energies (in MeV) as shown in Table 6.

Table 6. Pairing excitation energies (in MeV) for even-even  $^{18-26}\text{O}$  calculated from Eqs. (11)–(16)

$\zeta$	$k = 1$	$k = 2$	$k = 3$	$k = 4$	$k = 5$	$k = 6$
0	-12.60	-24.15	-31.12	-37.94	-37.82	-34.77
1	-8.10	-19.27	-26.75	-29.92	-27.14	—
2	0.62	-11.26	-21.60	-27.95	-25.21	—
3	—	-7.63	-17.51	-18.76	—	—
4	—	2.41	-9.24	-16.02	—	—
5	—	—	-4.77	—	—	—

One can assume a separable strength pairing (SSP) interaction,  $c_{jj'} = c_j c_{j'}^*$ . Though strong, this assumption is physically motivated because it links the pair-pair interaction strength to the individual pair formation probability. Furthermore, it is expected to be better than the equal strength pairing (ESP) approximation for which  $c_{jj'} = |G|$  for all orbitals. In this case, the corresponding Bethe ansatz equations can be simplified, which was reported in [28]. In Fig. 2, even-odd mass differences for Ni isotopes calculated by the general pairing (GP), separable strength pairing (SSP), and equal strength pairing (ESP), respectively, are plotted, which shows the SSP is indeed a good approximation to the nuclear pairing problem. In our calculation, the  $2p_{3/2}$ ,  $1f_{5/2}$ , and  $2p_{1/2}$  single-particle energies are taken from the experimental spectrum of  $^{57}\text{Ni}$  with  $\varepsilon_{3/2} = 0$ ,  $\varepsilon_{1/2} = 1.113$ , and  $\varepsilon_{5/2} = 0.769$  MeV. The parameters  $c_{jj'}$  (in MeV) in the GP case are obtained from the effective two-

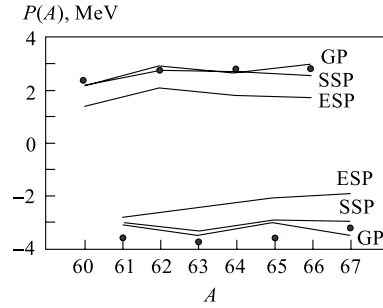


Fig. 2. Even-odd mass difference  $P(A) = E(A) + E(A-2) - 2E(A-1)$  for Ni isotopes calculated by the GP, SSP, and ESP, respectively, where  $E(A)$  is the total binding energy, and dots are the experimental quantities

body matrix given by [31], which yields  $c_{\frac{1}{2}\frac{1}{2}} = 0.89$ ,  $c_{\frac{3}{2}\frac{3}{2}} = 0.46$ ,  $c_{\frac{5}{2}\frac{5}{2}} = 0.58$ ,  $c_{\frac{1}{2}\frac{3}{2}} = 0.69$ ,  $c_{\frac{1}{2}\frac{5}{2}} = 0.32$ ,  $c_{\frac{3}{2}\frac{5}{2}} = 0.46$ . In the SSP calculation, the parameters  $c_j$  were determined as follows: Firstly, calculate the seniority zero one-pair ground state wave function,  $|k=1\rangle = \sum_j c'_j S_j^+ |0\rangle$ , from the  $J=0$  two-body pairing Hamiltonian *without* single-particle terms in the GP case. Then, reconstruct the SSP two-body part  $H_{\text{pairing}}^{\text{SSP}} = -\sum_{jj'} c_j c_{j'}^* S_j^+ S_{j'}^-$ , where  $c_j = \sqrt{g} c'_j$  and  $g$  is a real parameter, using the generalized pairing operator  $\sum_j c'_j S_j^+$  as done in [27], which should reproduce the seniority zero one-pair ground state energy derived in the GP case. This yields  $c_{1/2} = 0.75$ ,  $c_{3/2} = 0.68$ , and  $c_{5/2} = 0.65$ . And finally, the pairing strength in the ESP is taken from [32,33], which gives  $|G| = 0.33$  MeV.

**2.2. Nearest-Level Pairing Approximation for Well-Deformed Nuclei.** As shown previously, the Bethe ansatz approach to exact solutions of the mean-field plus general pairing requires one to solve a large number of nonlinear equations. Such a procedure is not practical when the number of levels and valence nucleon pairs are large, which is usually the case for well-deformed nuclei. Recently, a hard-core Bose–Hubbard model was proposed [2], which is equivalent to a mean-field plus nearest-level pairing theory. As is well known, an equal strength pairing interaction, which is used in many applications, is not a particularly good approximation for well-deformed nuclei. In [34], a level-dependent Gaussian-type pairing interaction with

$$G_{ij} = A e^{-B(\epsilon_i - \epsilon_j)^2} \quad (17)$$

was used, where  $i$  and  $j$  each represent doubly occupied levels with single-particle energies  $\epsilon_i$  and  $\epsilon_j$ . The parameters  $A < 0$  and  $B > 0$  are adjusted in such a way that the location of the first excited eigensolution lies approximately at the same energy as for the constant pairing case. Of course, there is some freedom in adjusting the parameters, allowing one to control in a phenomenological way the interaction among the levels. Expression (17) implies that scattering between particle pairs occupying levels with single-particle energies that lie close are favored; scattering between particle pairs in levels with distant single-particle energies are disfavored. As an approximation, this pairing interaction was further simplified to the nearest-level coupling, namely,  $G_{ij}$  is given by (17) if the levels  $i$  and  $j$  lie adjacent to one another in energy, with  $G_{ij}$  taken to be 0 otherwise. Hence, the Hamiltonian can be expressed as

$$\hat{H} = \sum_i \epsilon_i + \sum'_{i,j} t_{ij} b_i^+ b_j, \quad (18)$$

where the first sum runs over the orbits occupied by a single fermion which occurs in the description of odd- $A$  nuclei or broken pair cases, and the second primed

sum runs only over levels that are occupied by pairs of fermions. For the nearest-level pairing interaction case the  $t$ -matrix is given by  $t_{ii} = 2\epsilon_i + G_{ii} = 2\epsilon_i + A$  and  $t_{ii+1} = t_{i+1i} = G_{ii+1}$  with  $t_{ij} = 0$  otherwise. The fermion pair operators in this expression are given by

$$b_i^+ = a_i^+ a_{\bar{i}}^+, \quad b_i = a_{\bar{i}} a_i, \quad (19)$$

where  $a_i^+$  is the  $i$ th level single-fermion creation operator and  $a_{\bar{i}}^+$  is the corresponding time-reversed state. The Nilsson Hamiltonian is used to generate the mean-field. In this case there is at most one valence nucleon pair or a single valence nucleon in each level due to the Pauli principle. Equivalently, these pairs can be treated as bosons with projection onto the subspace with no doubly occupied levels.

The eigenstates of (18) for  $k$ -pair excitation can be expressed as

$$|k; \xi, (n_{j_1}, n_{j_2}, \dots, n_{j_r}) n_f\rangle = \sum'_{i_1 < i_2 < \dots < i_k} C_{i_1 i_2 \dots i_k}^{(\xi)} \times \\ \times b_{i_1}^\dagger b_{i_2}^\dagger \dots b_{i_k}^\dagger |(n_{j_1}, n_{j_2}, \dots, n_{j_r}) n_f\rangle, \quad (20)$$

where  $j_1, j_2, \dots, j_r$  are the levels occupied by  $r$  single particles, the prime indicates that  $i_1, i_2, \dots, i_k$  cannot be taken to be  $j_1, j_2, \dots, j_r$  in the summation, and  $n_f$  is the total numbers of single valence nucleons, that is  $n_f = \sum_j n_j$ . Since only even-even and odd- $A$  nuclei are treated without including broken pair cases in this paper,  $r$  is taken to be 1 for odd- $A$  nuclei, and 0 for even-even nuclei. In Eq. (20),  $C_{i_1 i_2 \dots i_k}^{(\xi)}$  is a determinant given by

$$\begin{vmatrix} g_{i_1}^{\xi_1} & g_{i_2}^{\xi_1} & \dots & g_{i_k}^{\xi_1} \\ g_{i_1}^{\xi_2} & g_{i_2}^{\xi_2} & \dots & g_{i_k}^{\xi_2} \\ \dots & \dots & \dots & \dots \\ g_{i_1}^{\xi_k} & g_{i_2}^{\xi_k} & \dots & g_{i_k}^{\xi_k} \end{vmatrix}, \quad (21)$$

where  $\xi$  is a shorthand notation for a selected set of  $k$  eigenvalues of the  $t$  matrix without the corresponding  $r$  rows and columns denoted as  $\tilde{t}$ , which can be used to distinguish the eigenstates with the same number of pairs,  $k$ , and  $g^{\xi_p}$  is the  $p$ th eigenvector of the  $\tilde{t}$  matrix.

The excitation energies corresponding to (20) can be expressed as

$$E_k^{(\xi)} = \sum_{i=1}^r \epsilon_{j_i} + \sum_{j=1}^k E^{(\xi_j)}, \quad (22)$$

where the first sum runs over  $r$  Nilsson levels, each occupied by a single valence nucleon, which occurs in odd- $A$  nuclei or in broken pair cases; the second one is a sum of  $k$  different eigenvalues of the  $\tilde{t}$  matrix. Obviously,  $\tilde{t}$  is a  $(k-r) \times (k-r)$  matrix, since those orbits occupied by single valence nucleons are excluded resulting from the Pauli blocking.  $E^{(\xi_p)}$  is the  $p$ th eigenvalue of the  $\tilde{t}$ -matrix, that is

$$\sum_j \tilde{t}_{ij} g_j^{\xi_p} = E^{(\xi_p)} g_i^{\xi_p}. \quad (23)$$

Hence

$$\begin{aligned} \hat{H}|k; \xi, (n_{j_1}, n_{j_2}, \dots, n_{j_r})n_f\rangle &= \\ &= \sum_{i_1 < i_2 < \dots < i_k} \sum_{\mu=1}^k \sum_P (-)^P \left( \sum_{i=1}^r \varepsilon_{j_i} + E^{(\xi_{P(\mu)})} \right) \times \\ &\times g_{i_1}^{(\xi_{P(1)})} g_{i_2}^{(\xi_{P(2)})} \dots g_{i_\mu}^{(\xi_{P(\mu)})} \dots g_{i_k}^{(\xi_{P(k)})} b_{i_1}^\dagger b_{i_2}^\dagger \dots b_{i_k}^\dagger |(n_{j_1}, n_{j_2}, \dots, n_{j_r})n_f\rangle = \\ &= E_k^{(\xi)} |k; \xi, (n_{j_1}, n_{j_2}, \dots, n_{j_k})n_f\rangle, \quad (24) \end{aligned}$$

where  $P$  runs over all permutations;  $E^{(\xi_\mu)}$  is the  $\mu$ th eigenvalue of the  $\tilde{t}$  matrix. Eq. (22) is valid for any  $k$ . If one assumes that the total number of orbits is  $N$  for even-even nuclei, the  $k$ -pair excitation energies are determined by the sum of  $k$  different eigenvalues chosen from the  $N$  eigenvalues of the  $\tilde{t}$  matrix with  $r = 0$ , the total number of excited levels is  $N!/k!(N-k)!$ . While for odd- $A$  nuclei or broken pair cases, the levels that are occupied by the single valence nucleons should be excluded in the original  $t$  matrix. In the latter case, the eigenvalue problem (18) can be solved simply by diagonalizing the corresponding  $\tilde{t}$  matrix as shown in Eq. (22).

Nuclei in the rare-earth and actinide regions are fitted by the mean-field plus nearest-level pairing model using the axial-symmetric Nilsson potential as the mean-field. In this case, exact solutions can be obtained by using the above simple method. As for the binding energy, the contributions from the real quadrupole-quadrupole interaction are expected to be relatively small [35]. This conclusion applies to low-lying  $0^+$  excited states as well as ground states. As shown in [36], contributions from the pairing interaction are very important to the low-lying excited  $0^+$  states in these deformed regions. Hence, the position of low-lying  $0^+$  states is an estimate based on the Nilsson mean-field plus pairing approximation. As examples, binding energies and low-lying  $0^+$  states of  $^{226-234}\text{Th}$ ,  $^{230-240}\text{U}$ , and  $^{236-243}\text{Pu}$  isotopes were fitted. Table 7 shows the binding energy results as well as pairing excitation energies of the theory for  $^{226-234}\text{Th}$ ,  $^{230-240}\text{U}$ , and

Table 7. Calculated binding and pairing excitation energies are compared with the corresponding experimental values for various  $^{226-234}\text{Th}$ ,  $^{230-240}\text{U}$ , and  $^{236-243}\text{Pu}$  isotopes.  $B_{\text{th}}$  and  $B_{\text{exp}}$  denote, respectively, the theoretical and experimental binding energies [37]

Nucleus	Spin and parity	$B_{\text{exp}}$ , MeV	$B_{\text{th}}$ , MeV	Pairing excitation			
				Energies of exp., MeV		Energies of th., MeV	
$^{226}\text{Th}$	$0^+$	-1730.54	-1732.17	$0_2^+$	0.805	$0_2^+$	0.999
				$1^+$	3.226	$1^+$	1.299
$^{227}\text{Th}$	$\frac{1^+}{2}$	-1736.00	-1733.97	$2_2^+$	5.188	$2_2^+$	1.391
				$1^+$	6.495	$1^+$	1.415
$^{228}\text{Th}$	$0^+$	-1743.10	-1739.30	$2_3^+$	0.831	$2_3^+$	0.718
				$1^+$	0.029	$1^+$	0.057
$^{229}\text{Th}$	$\frac{5^+}{2}$	-1748.36	-1744.42	$2_2^+$	0.317	$2_2^+$	0.516
				$5^+$	0.635	$5^+$	1.199
$^{230}\text{Th}$	$0^+$	-1755.16	-1756.90	$2_3^+$	0.241	$2_3^+$	0.907
				$5^+$	0.302	$5^+$	1.204
$^{231}\text{Th}$	$\frac{5^+}{2}$	-1760.27	-1764.21	$2_2^+$	0.317	$2_2^+$	1.230
				$5^+$	0.730	$5^+$	1.647
$^{232}\text{Th}$	$0^+$	-1766.71	-1768.66	$0_2^+$	1.079	$0_2^+$	2.585
				$0_3^+$	0.310	$0_3^+$	0.907
$^{233}\text{Th}$	$\frac{1^+}{2}$	-1771.50	-1772.92	$1^+$	0.810	$1^+$	1.066
				$2_2^+$	1.150	$2_2^+$	2.562
$^{234}\text{Th}$	$0^+$	-1777.69	-1779.81	$0_3^+$	1.470	$0_3^+$	2.904
				$0_4^+$	—	$0_4^+$	—
$^{231}\text{U}$	$\frac{5^-}{2}$	-1758.72	-1761.26	—	—	$5^-$	0.646
$^{232}\text{U}$	$0^+$	-1760.00	-1758.94	$2_2^+$	0.691	$2_2^+$	0.961
				$5^+$	0.340	$5^+$	0.732
$^{233}\text{U}$	$\frac{5^+}{2}$	-1771.74	-1770.23	$2_2^+$	0.546	$2_2^+$	0.803
				$5^+$	0.809	$5^+$	0.747
$^{234}\text{U}$	$0^+$	-1778.59	-1774.41	$2_3^+$	1.044	$2_3^+$	0.933
				$0_2^+$	1.781	$0_2^+$	1.696
				$0_4^+$	0.670	$0_4^+$	0.826
				$7^-$	—	$7^-$	—
				$2_2^-$	—	$2_2^-$	—

End of Table 7

Nucleus	Spin and parity	$B_{\text{exp}}$ , MeV	$B_{\text{th}}$ , MeV	Pairing excitation			
				Energies of exp., MeV		Energies of th., MeV	
$^{235}\text{U}$	$\frac{7^-}{2}$	-1783.89	-1780.23	$\frac{7^-}{2_3}$	0.700	$\frac{7^-}{2_3}$	1.056
$^{236}\text{U}$	$0^+$	-1790.44	-1786.71	$0_2^+$	0.919	$0_2^+$	0.913
				$0_3^+$	2.155	$0_3^+$	1.186
				$0_4^+$	2.750	$0_4^+$	2.319
				$1^+$	0.846	$1^+$	0.586
$^{237}\text{U}$	$\frac{1^+}{2}$	-1795.56	-1795.48	$\frac{2_2^+}{1^+}$	0.905	$\frac{1^+}{2_2}$	0.700
$^{238}\text{U}$	$0^+$	-1801.715	-1802.22	$0_2^+$	0.925	$0_2^+$	0.877
				$0_3^+$	0.993	$0_3^+$	2.874
				$5^+$	0.193	$5^+$	0.185
$^{239}\text{U}$	$\frac{5^+}{2}$	-1806.52	-1810.23	$\frac{2_2^+}{5^+}$	0.734	$\frac{2_2^+}{5^+}$	0.459
				$\frac{2_3^+}{5^+}$	0.757	$\frac{2_3^+}{5^+}$	0.786
$^{240}\text{U}$	$0^+$	-1812.45	-1815.41	$2_4^-$	—	$0_2^+$	0.100
$^{236}\text{Pu}$	$0^+$	-1790.46	-1792.36	$0_2^+$	3.000	$0_2^+$	0.645
				$7^-$	0.691	$7^-$	0.617
$^{237}\text{Pu}$	$\frac{7^-}{2}$	-1795.56	-1795.87	$\frac{2_2^-}{7^-}$	0.696	$\frac{2_2^-}{7^-}$	2.173
				$2_3^-$	0.942	$0_2^+$	0.407
$^{238}\text{Pu}$	$0^+$	-1801.72	-1799.96	$0_3^+$	1.134	$0_3^+$	1.987
				$0_4^+$	1.229	$0_4^+$	2.170
				$0_5^+$	1.427	$0_5^+$	2.681
$^{239}\text{Pu}$	$\frac{1^+}{2}$	-1806.52	-1805.12	$1^+$	0.753	$1^+$	0.354
$^{240}\text{Pu}$	$0^+$	-1812.45	-1810.68	$\frac{2_2^+}{0_2^+}$	0.860	$\frac{2_2^+}{0_2^+}$	1.030
				$0_3^+$	1.089	$0_3^+$	2.144
				$0_4^+$	1.526	$0_4^+$	2.626
				$5^+$	0.233	$5^+$	0.088
$^{241}\text{Pu}$	$\frac{5^+}{2}$	-1816.64	-1816.09	$\frac{2_2^+}{5^+}$	0.801	$\frac{2_2^+}{5^+}$	0.587
$^{242}\text{Pu}$	$0^+$	-1822.41	-1821.89	$2_3^+$	0.956	$2_3^+$	1.186
				$7^-$	0.333	$7^-$	0.845
$^{243}\text{Pu}$	$\frac{7^-}{2}$	-1826.63	-1828.63	$\frac{2_2^-}{7^-}$	0.450	$\frac{2_2^-}{7^-}$	1.146
				$2_3^-$	0.742	$2_3^-$	1.815
				$2_4^-$	—	$2_4^-$	—

$^{236-243}\text{Pu}$ , with the corresponding experimental values taken from [37]. The parameters  $A$  and  $B$  in Eq.(17) were fit as follows to maximize agreement with experiment:

$$A = \alpha_1 + \beta_1 k + \gamma_1 n_f, \quad B = \alpha_2 + \beta_2 k + \gamma_2 n_f, \quad (25)$$

where  $\alpha_i$ ,  $\beta_i$ , and  $\gamma_i$  are parameters that were fit for each isotope.

**2.3. Conclusions Related to «Novel» Algebraic Approaches.** In conclusion, mean-filed plus general pairing interaction models are exactly solvable. In these cases the Bethe ansatz can be evoked, from which excitation energies and the corresponding wave functions can be determined through a set of nonlinear equations. These exact solutions are accessible for valence particle or hole pairs,  $k \leq 4$ . Therefore, the method can be applied to  $ds$  and  $fp$  shell nuclei. However, solving these nonlinear equations is not practical when the number of levels and valence nucleon pairs are large, which applies for well-deformed nuclei. In the latter case, a hard-core Bose–Hubbard model was adopted, which is equivalent to a mean-field plus nearest-level pairing theory. This model is also exactly solvable, and is applied to describe well-deformed nuclei in the rare-earth and actinide regions. Because of the exact solvability, many physical quantities, such as occupation number probabilities, moment of inertia, electromagnetic transition rates, as well as one-particle and two-particle transfer reaction rates can be calculated exactly, which will be reported elsewhere.

**Acknowledgements.** This work was supported by the U. S. National Science Foundation through a regular grant (9970769) and a Cooperative Agreement (9720652) that includes matching from the Louisiana Board of Regents Support Fund. Support from Conacyt (México) as well as the Natural Science Foundation of China (Grant No. 10175031) and the Science Foundation of the Liaoning Education Commission (Grant No. 990311011) is also acknowledged.

#### REFERENCES

1. *Beuschel T., Hirsch J. G., Draayer J. P.* // Phys. Rev. C. 2000. V. 61. P. 054307.
2. *Feng Pan, Draayer J. P.* // J. Phys. A: Math. Gen. 2000. V. 33. P. 1597.
3. *Sviratcheva K. D. et al.* // J. Phys. A: Math. Gen. 2001. V. 34. P. 8365.
4. *Dobes J.* // Phys. Lett. B. 1997. V. 413. P. 239.
5. *Macchiaveli A. O. et al.* // Phys. Lett. B. 2000. V. 480. P. 1.
6. *Kracíková T. I. et al.* // Phys. Rev. C. 1998. V. 58. P. 1986.
7. *Zamfir N. V. et al.* // Phys. Rev. C. 1999. V. 60. P. 054319.
8. *Lehmann H. et al.* // Phys. Rev. C. 1998. V. 57. P. 569.
9. *Börner H. G. et al.* // Phys. Rev. Lett. 1991. V. 66. P. 2837.
10. *Oshima M. et al.* // Nucl. Phys. A. 1993. V. 557. P. 635c.

11. *Draayer J. P., Popa G., Hirsch J. G.* // Acta Phys. Polon. B. 2001. V. 32. P. 2697.
12. *Popa G., Hirsch J. G., Draayer J. P.* // Phys. Rev. C. 2000. V. 62. P. 064313.
13. *Ring P., Schuck P.* The Nuclear Many-Body Problem. Berlin: Springer, 1979.
14. *Elliott J. P.* // Proc. Roy. Soc. A. 1958. V. 245. P. 128; 562.
15. *Casten R. F. et al.* Algebraic Approaches to Nuclear Structure: Interacting Boson and Fermion Models. N. Y.: Harcourt, Brace, and Jovanovich, 1993.
16. National Nuclear Data Centre. <http://bnlnd2.dne.bnl.gov>
17. *Ui H.* // Prog. Theor. Phys. 1970. V. 44. P. 153.
18. *Castanõs O., Draayer J. P., Leschber Y.* // Z. Phys. A. 1988. V. 329. P. 33.
19. *Cornwell J. F.* Techniques in Physics 7: Group Theory in Physics. Orlando, 1985. V. 2; 1988. V. 33.
20. *Rompf D. et al.* // Phys. Rev. C. 1998. V. 57. P. 1703.
21. *Beuschel T. et al.* // Ibid. P. 1233.
22. *Racah G.* // Phys. Rev. 1942. V. 62. P. 438; 1943. V. 63. P. 367;  
*Bohr A., Mottelson B. R., Pines D.* // Phys. Rev. 1958. V. 110. P. 936;  
*Belyaev S. T.* // Mat. Fys. Medd. 1959. V. 31. P. 11.
23. *Lane A. M.* Nuclear Theory. W. A. Benjamin Inc., 1964.
24. *Goodman A. L.* // Adv. Nucl. Phys. 1979. V. 11. P. 263.
25. *Engel J., Langanke K., Vogel P.* // Phys. Lett. B. 1996. V. 389. P. 211.
26. *Richardson R. W.* // Phys. Lett. 1965. V. 14. P. 325.
27. *Feng Pan, Draayer J. P., Ormand W. E.* // Phys. Lett. B. 1998. V. 422. P. 1.
28. *Feng Pan, Draayer J. P.* // Ibid. V. 442. P. 7.
29. *Feng Pan, Draayer J. P.* // Ann. Phys. (N. Y.). 1999. V. 271. P. 120.
30. *Wildenthal B. H.* // Prog. Part. Nucl. Phys. 1984. V. 11. P. 1.
31. *Auerbach N.* // Phys. Rev. 1967. V. 163. P. 1203.
32. *Kerman A. K., Lawson R. D.* // Phys. Rev. 1961. V. 124. P. 162.
33. *Kisslinger L. S., Sorensen R. A.* // Mat. Fys. Medd. Dan. Vid. Selsk. 1961. V. 32. P. 5.
34. *Molique H., Dudek J.* // Phys. Rev. C. 1997. V. 56. P. 1795.
35. *Nilsson S. G., Prior O.* // Mat. Fys. Medd. Dan. Vid. Selsk. 1961. V. 32. P. 1.
36. *Garret P. E.* // J. Phys. G. 2001. V. 27. P. R1.
37. *Moller P. et al.* // Atom. Data Nucl. Data Tables. 1995. V. 59. P. 185.